PAPER REF: 7101

FATIGUE STRENGTH OF CARBON STEEL COVERED WITH PROTECTIVE LAYERS FOR CO_2 ASSISTED SHALE GAS MINING

Marta Baran, Tomasz Brynk[(*)], Zbigniew Pakiela
Faculty of Materials Science and Engineering, Warsaw University of Technology, Warsaw, Poland
[(*)]*Email:* tbrynk@inmat.pw.edu.pl

ABSTRACT

In this study, fatigue behavior of samples with Inconel 625 and 304 stainless steel protective coating deposited on P110 steel used as casing tube material in a natural gas wells has been investigated. Loading conditions of well operation were simulated by 3-point bending dynamic tests which were carried out on mini-samples (34,2 x 7,6 x 3,8 mm). The S-N curves estimated for both protective coating systems and strain distribution maps derived by Digital Image Correlation (DIC) were referred to base metal results. Abovementioned mechanical tests were supplemented by SEM observations of fractures and micro CT scans that enabled to estimate coating thickness and determine the effect of their quality on fatigue behavior. Presented investigation confirmed good adhesion between coatings and base material, nevertheless revealed also discontinuities in the Inconel coating, which substantially affected results of fatigue tests. The life to failure of deposited material was shorter in comparison to unmodified P110 steel, however modification of cladding technology leading to decrease in quantity of defects might make P110 steel with weld cladded Inconel 625 competitive in relation to P110 steel to a certain extent of loadings.

Keywords: fatigue, Digital Image Correlation (DIC), anticorrosion coating, shale gas.

INTRODUCTION

The modern mining industry is expected to both, discover new deposits of mineral resources and minimize the exploration impact on the natural environment. The technology that enables sequestration of shale gas reservoirs together with simultaneous anthropogenic-sourced gases deposition is liquid/supercritical CO_2 injection as a fracking fluid. However, carbon dioxide environment significantly affects carbon steels, which are extensively used in oil and gas industry because of economic aspects. To date, great attention was devoted to the mechanism of CO_2 corrosion due to both the presence of its large quantity in deep gas reservoirs and possibility of its application in well stimulation. Thermodynamic transformation resulted from natural heating of CO_2 on a few kilometers depth under earth surface induces pressure suitable for shale rock formation fracturing (Niezgoda, 2013).

Application of steels listed in API 5CT, generally used as a casing or tubing pipe materials with P110 being a prominent example, is limited by their corrosiveness in wet CO_2 environment, nevertheless, they might be modified by anticorrosion coatings deposition. Over recent years several researches were published on corrosion behavior of P110 steel without (Bao, 2016; Xie, 2015 and Yin, 2011) and with anticorrosion coatings (Lin, 2015 and Lin, 2011). However, it should be noted that the surface condition is included to factors

affecting fatigue strength of materials. Therefore, an implementation of a new material-coating system ought to be preceded by fatigue tests (Revie, 2015; Zhao, 2016 and Hong, 2015).Comparison of materials by determination of the time to failure is possible on the base of S-N curves which present relationship between the magnitude of a cyclic stress (S) and number of cycles to failure (N).The representation of tensile hoop stresses occurring in pipes during exploitation could be obtained by bending test (Revie, 2015) (Figure 1).

In this study fatigue of P110 steel as a reference material and P110 with weld cladded Inconel 625 and austenitic stainless steel has been investigated.The S-N curves were obtained for them in 3-point bending test of miniaturized samples. All fatigue tests were preceded by Computer Tomography (CT) scans aiming to verification of potential welding defects and coating thickness measurement. Moreover, dynamic tests were supplemented by strain distribution maps obtained by Digital Image Correlation (DIC) and Scanning Electron Microscopy (SEM) of fracture surfaces.
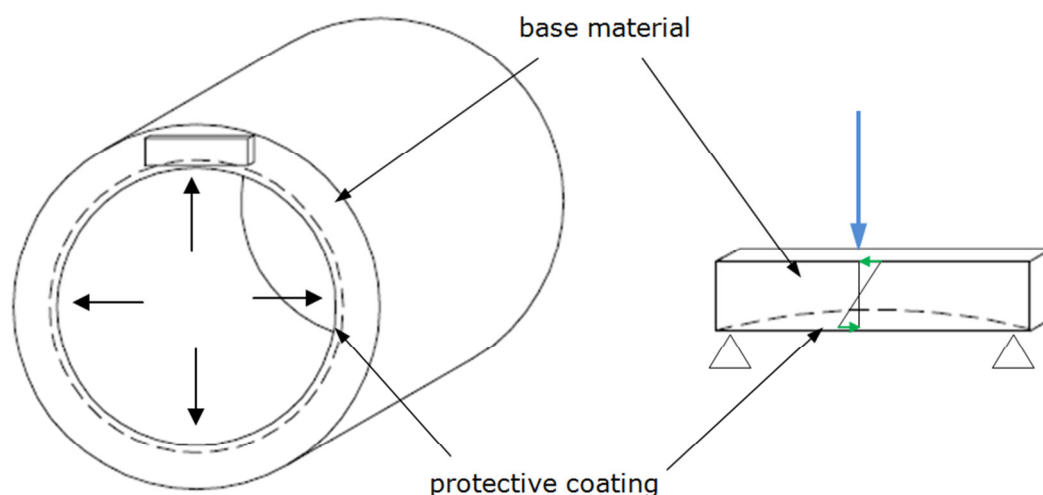

Fig. 1 - The scheme of 3-point bending specimen location relative to pipe.

EXPERIMENTAL METHODOLOGY

Materials

The material subjected to the research was P110 steel, which the chemical composition is listed in Table 1. The average ultimate tensile strength (UTS) and yield strength (YS) are shown in Table 2.

Table 1 - Chemical composition of P110 steel investigated in this studycompared to API 5CT

Element	C	Si	Mn	P	S	Fe
Content (wt. %)	0.243	0.196	0.990	0.014	0.002	Bal
API 5CT	-	-	-	max 0.030	max 0.030	-

Table 2 - Mechanical properties of P110 steel investigated in this work compared to API 5CT

		UTS	YS
		MPa	MPa
investigated P110 steel		926	870
API 5CT	**min**	862	758
	max	-	965

Besides of the initial state described in Table 1 and 2, tests were carried out on P110 steel cladded with Inconel 625 and 304 stainless steel. The mechanical properties estimated for used coating materials are shown in Table 3.

Table 3 - Estimated mechanical properties of protective coatings materials (Gale, 2004)

	UTS	YS
	MPa	MPa
Inconel 625 (annealed)	930	520
Inconel 625 (solution treated)	810	325
304 (softened)	480	230

Samples preparation

Samples for 3-point bending with 34,2 x 7,6 x 3,8 mm dimensions are schematically shown in Figure 1, where protective coating is marked by a dotted line. Samples dimension and specific shape of coating were determined by specimen location relative to pipe. To minimize probability of protective coating damaging specimens were cut by technology of wire electrical discharge machining (WEDM) and then were ground up to 1200 grit. In order to subsequent strain fields measurements using DIC front surfaces of specimens were sprayed white and black paint to obtain a speckle pattern.

Fatigue tests

Fatigue tests in 3-point bending mode were done for three series of samples: P110 steel in the initial state and with Inconel 625 and austenitic stainless steel protective coating. Applied magnitude of loading was lower than yield strength obtained in static 3-point bending tests ensuring high cycle fatigue conditions. Loading cycles have a sinusoidal shape, the frequency of 20 Hz and cycle asymmetry ratio R=0.1. All the fatigue specimens were tested at room temperature to the point of fracture excepting the lack of failure to 1.5million cycles when tests were interrupted.

Fatigue tests were conducted by using horizontal testing machine equipped with MTS hydraulic actuator and force transducer with +/- 15kN loading range.

Fatigue tests with DIC

All the fatigue tests were conducted with 2D DIC measurements. Trigger of the camera observing front surface of samples was synchronized with the maximum compressive load. Every 250th image was registered for further analyzes. Strain distribution maps processing was made utilizing Vic2D software (Correlated Solutions, USA).

Complementary tests

CT scans were made directly after cutting and before grinding by means of MicroXCT-400 High Resolution X-Ray Imagine System. Fractographic observations were conducted employing scanning electron microscope Hitachi S-3500N.

RESULTS AND DISCUSSION

The summarized results describing quality of weld cladding coating are presented in Tables 4 and 6. For all the specimens with anticorrosive coatings the coefficient of defectiveness *d* was assigned. This parameter, based on welding standard (ISO 5817:2014 and ISO 6520-1:2007), is equal to the area's ratio of revealed with CT scans discontinuities to the entire coating area. It should be noted that *d* coefficient has only qualitative meaning. It was determined based on the blurry contours of defects. Thus, it is dependent on a subjective assessment of grey levels.

The differences in dimensions and shape of defects for both coating are clearly visible. Discontinuities are significantly larger in the case of Inconel 625, however, it should be noticed that for both coating they occur near the interface boundary between the core material and the coating as well as they are characterised by blunted edges.

Table 4 - Results of fatigue tests and CT scans of investigated specimens.

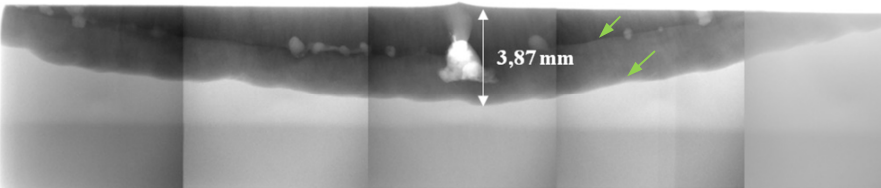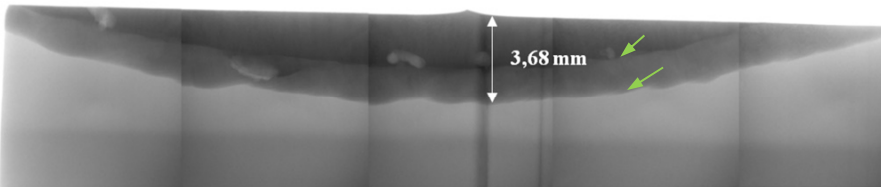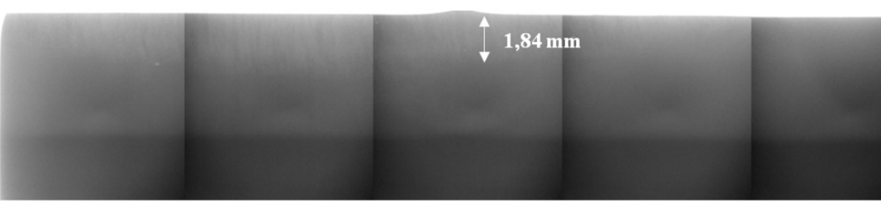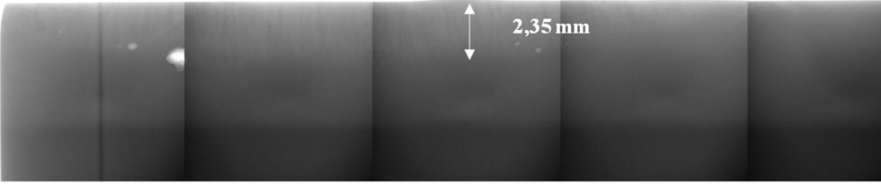| Cladded material	No. of specimen	Coefficient of coatings defectiveness *d* [%]	Thickness of coatings *t* [mm]	Maximum bending stress during loading cycle σ_{max}* [MPa]	Cycles to failure
base material without coating	1	-	-	1300	47 657
	2			1100	98 060
	3			900	254 661
	4			850	378 514
	5			800	1 500 000**
	6			700	1 500 000**
Inconel 625	1	6,89	3,87	850	12 050
	2	0,00	2,63	825	503 908
	3	4,11	3,05	800	43 135
	4	0,17	2,89	775	453 555
	5	3,16	3,68	750	429 891
	6	1,11	3,00	650	1 500 000**
304 steel	1	0,22	2,11	900	87 544
	2	0,09	1,84	850	142 703
	3	0,45	2,00	750	149 512
	4	0,52	1,07	700	172 229
	5	1,21	2,35	650	969 176
	6	0,12	2,18	600	1 500 000**
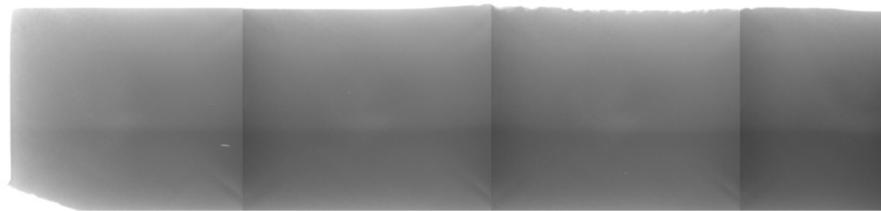
* Bending stress is defined by equation: $\sigma = M/W$, where M - bending moment and W - flexural modulus.
** The failure didn't occur until 1,5 million cycles. Test interrupted.

Moreover, obtained images (Table 5) do not permit to determine the nature of discontinuities. They only visualize materials density changes on the X-ray way, thus inclusions of a density lower than density of steel could resemble porosity.

The coating thickness changes (Table 4) resulted from overlay technology in which coatings thickness varies according to length of a pipe axis. Lines pointed by arrows (Table 5 - Inconel 625, no. 1 and no. 5) indicate thickness changes in each specimen and correspond to minimal and maximal thickness of coating. The changes of the same nature occur in stainless steel coatings, but they remain invisible on CT scans because of almost equal density of coating and core material. Observations based on CT scans are confirmed by fracture surface illustration (Figure 2).

Table 5 - CT scans of selected specimens.

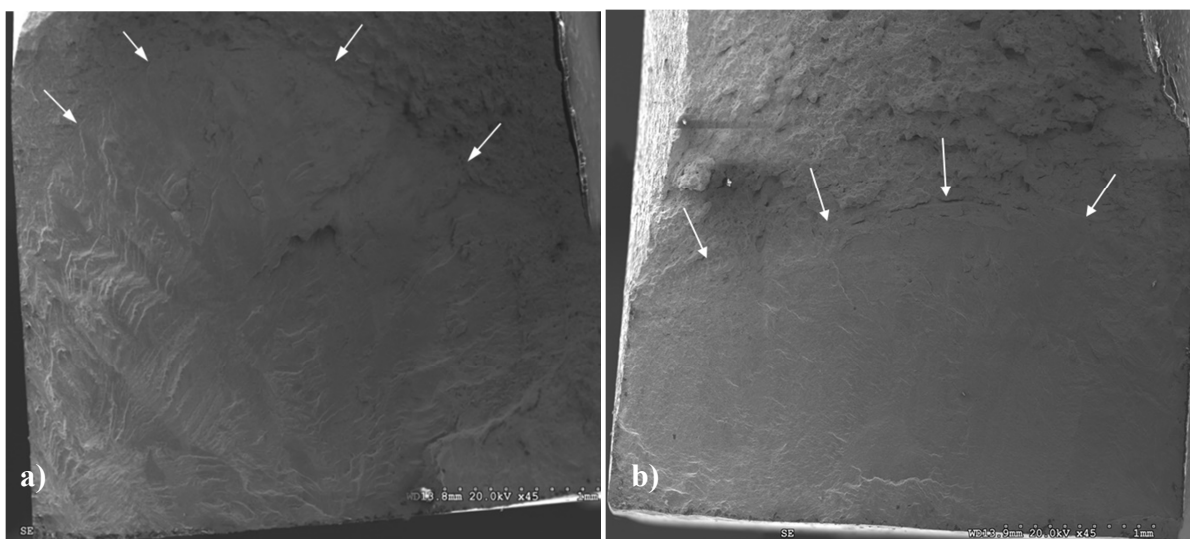| Cladded material	No. of specimen	CT scan
Base material without coating	1	
Inconel 625	1	3,87 mm
	5	3,68 mm
304 steel	2	1,84 mm
	5	2,35 mm

Fig. 2 - Fracture surfaces of saples with a) Inconel 625 coating - specimen no. 4 - loaded with maximal stress 775 MPa, b) 304coating - specimen no. 3 -loaded with maximal stress 750 MPa (coating -base material intrfaces marked with white arrows)

The results concerning fatigue strength of unmodified P110 steel compared to samples with anticorrosion coatings are presented in Table 4 and graphically in Figure 3. The fatigue limit of P110 steel for 3-point bending test is estimated to 800 MPa while weld cladded samples were characterized by lower number of cycles to failure for corresponding load levels. The results obtained for the stainless steel coating with regard to the base material were figured below P110 steel over the all loading range. Two specimens with the higher coefficient of defectiveness from Inconel 625 cladded group showed reduced number of cycles to failure due to decrease of loaded cross-section area and increase of stress concentration.
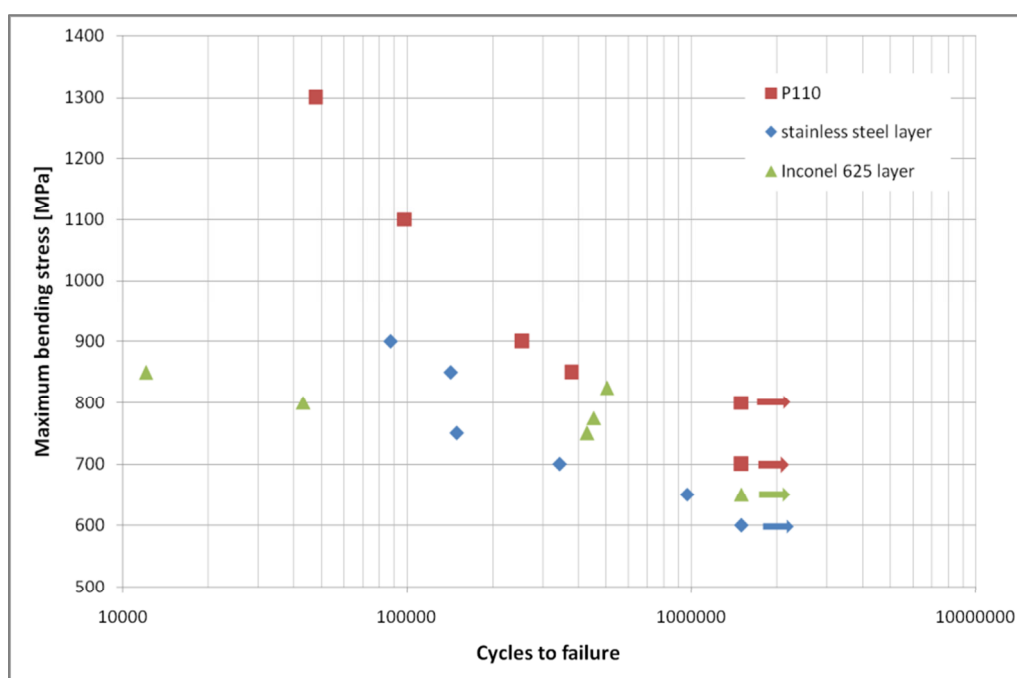

Fig. 3 - Wohler's curves for samples without and with anticorrosive coatings (3-point bending, R=0.1, f=20 Hz).
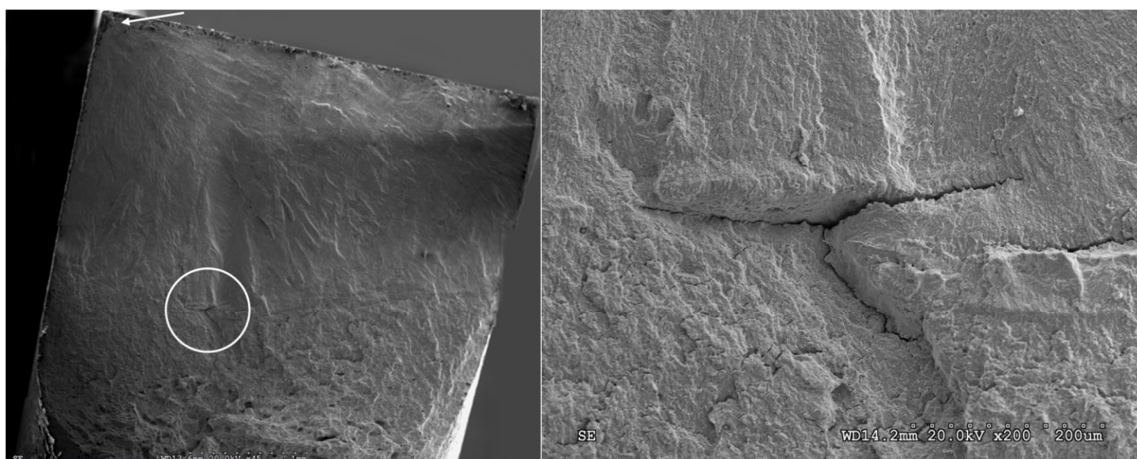
Fig. 4 - SEM fractography of the fatigue specimen with austenitic stainless steel coating - no. 5 (maximal bending stress: 650 MPa, cycles to failure 969 176) (a) fatigue fracture; (b) delamination between the coating and the core material

Fractography observations for the all specimens with austenitic stainless steel indicate small delaminations between the coating (circled area) and the base material, which were shown in Figures 4 and 5. Nevertheless, origins of fractures were localized in the specimens corners in all cases (pointed by arrows). Moreover, strain localizations on the coating boundary were not registered on strain distribution maps (Figure 6).
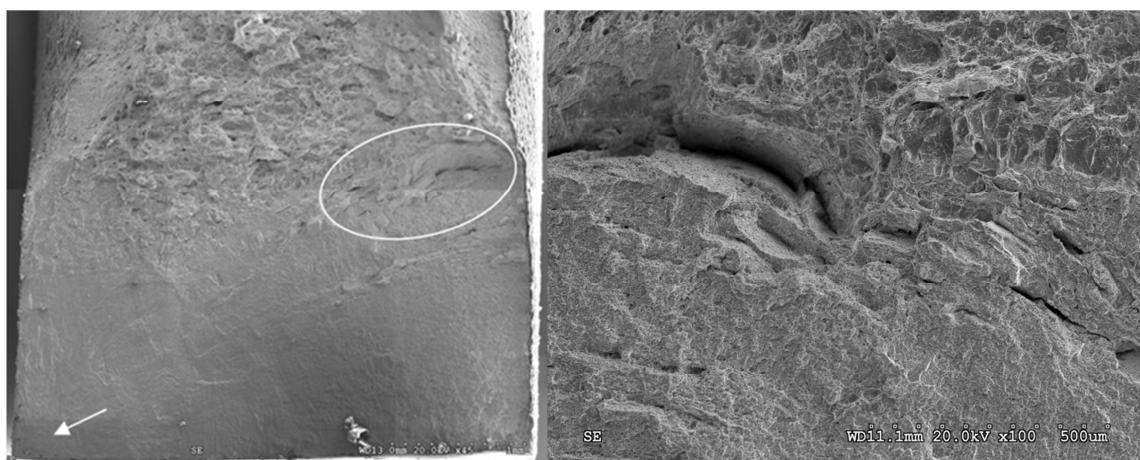

Fig. 5 - SEM fractography of the fatigue specimen with austenitic stainless steel - no. 1 (maximal bending stress: 900 MPa, cycles to failure 87 544) (a) fatigue fracture; (b) delamination between the coating and the core material

The substantial strain localization in specimens no. 1 and 2 (coated withstainless steel) was observed in the first few hundred loading cycles (Figure 7) reaching the value equal to approximately 4% after 500 cycles. The mentioned effect could by caused by significant difference between yield strenghts of core and coating material (Tables 2 and 3) and microstructural changes in P110 steel as a result of heating during weld overlaying. The coating deposition caused significant gradient of hardness in pipe cross-sections at depth of approximately 7 mm and its decrease compared to P110 steel which average value is equal 309 HV_1 (Figure 8). Phase transition induced by heat is also confirmed by microstructural observation where original sorbite was transformed in ferritic perlitic structure in case of samples with both types of coating (Figure 9). Abovementioned effect of early strain

localization was not observed in case of samples with the nickel-based alloy coating and P110 without coating loaded with highest stress levels (Figure 7).
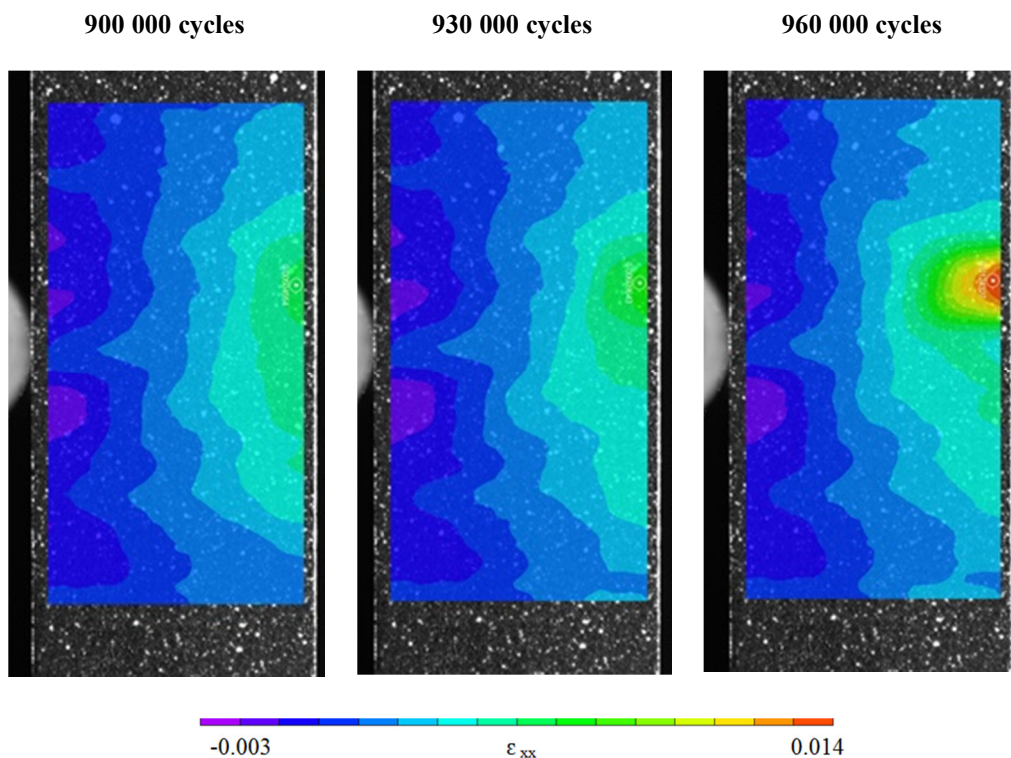
900 000 cycles   **930 000 cycles**   **960 000 cycles**

Fig. 6 - Strain distribution mapsof the fatigue specimen with austenitic stainless steel - no. 5 (maximal bending stress: 650 MPa, cycles to failure 969 176).
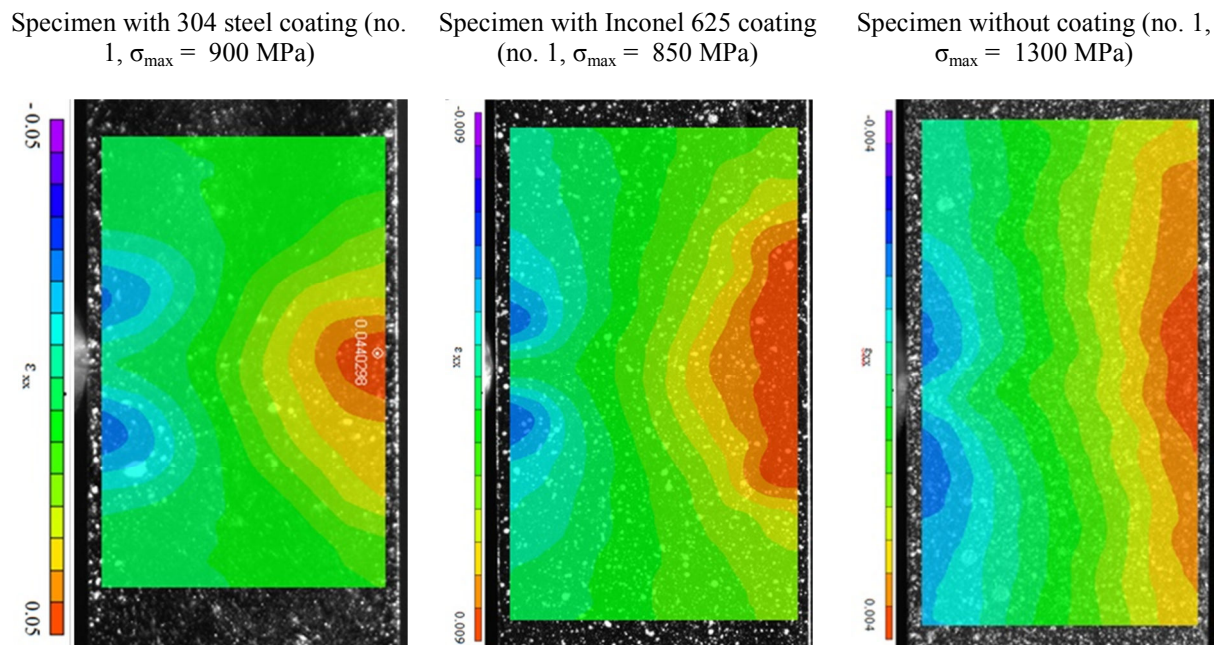
Specimen with 304 steel coating (no. 1, σ_{max} = 900 MPa)   Specimen with Inconel 625 coating (no. 1, σ_{max} = 850 MPa)   Specimen without coating (no. 1, σ_{max} = 1300 MPa)

Fig. 7 - Strain distribution mapsof the fatigue specimen after 500 cycles of loading.
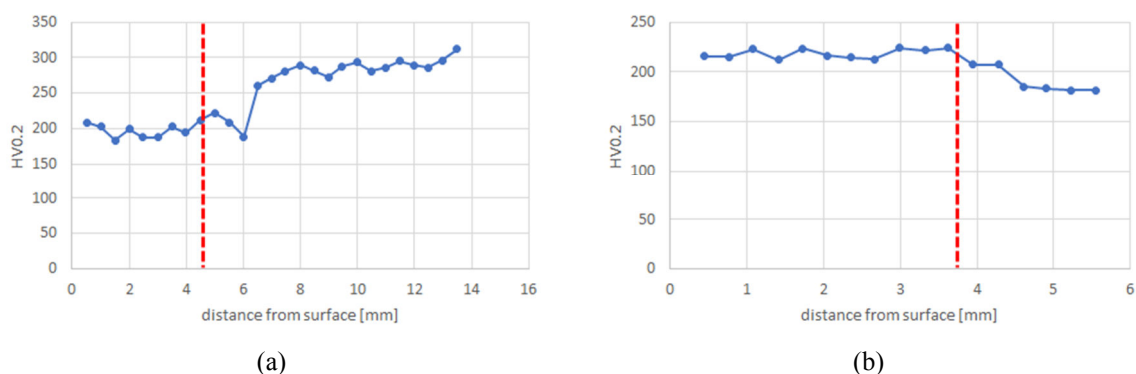
| (a) | (b) |

Fig. 8 - Hardness profiles for (a) P110 cladded with Inconel 625; (b) P110 cladded with stainless steel (coating interfaces marked with red dotted lines).

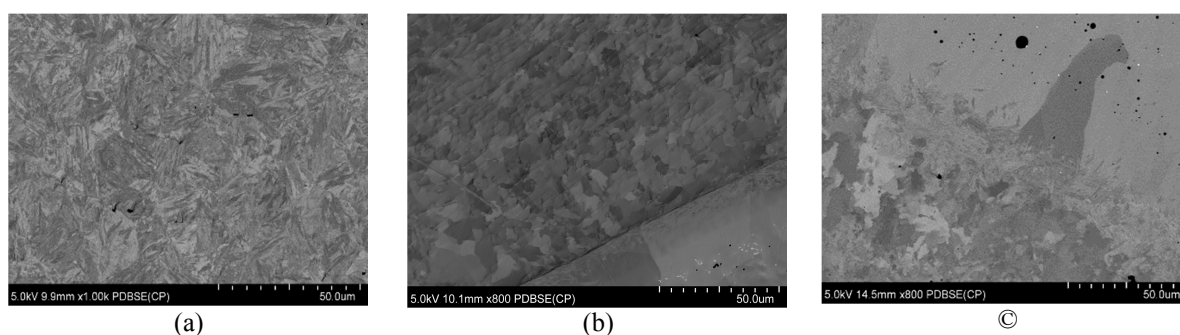| (a) | (b) | © |

Fig. 9 - Microstructure of (a) P110 steel without coating; (b) P110 - Inconel 625 coating interface (P110 at top); (c) P110 - stainless steel interfce (P110 at botom)

CONCLUSIONS

The fatigue performance depicts that specimens with weld cladding austenitic stainless steel performed worst compared to the core material. Complementary tests did not indicate the minor discontinuities influence on fatigue tests results. The mainly reason for obtained performance are both changes in core material microstructure caused by weld overlaying and significantly lower yield strength of the anticorrosive coating in relation to P110 steel.

Large defects revealed on the interface of investigated nickel-based alloy coating and core material cause decrease of effective cross-sections areas, and therefore the worst fatigue performance. Moreover, microstructural changes due to weld heating negatively affect fatigue test results.

Part of samples with nickel-based alloy coating showed higher number of cycles to failure than steel coating. Based on the above, further research on Inconel 625 coating are planned in order to compare results obtained for specimens with defects to specimens without discontinuities.

ACKNOWLEDGMENTS

REFERENCES

[1] Bao M, Ren Ch, Lei M, Wang X, Singh A, Guo X. Electrochemical behaviour of tensile stressed P110 steel in CO_2 environment. Corrosion Science, 2016, 112, pp. 585-595.

[2] Gale WF, Totemeier TC. Smithells Metals Reference Book (Eighth Edition), 2004.

[3] Hong SW, Koo JM, SeokChS, Kim JW, Kim JH. Fatigue life prediction for an API 5L X42 natural gas pipeline. Engineering Failure Analysis, 2015, 56, pp. 396-402.

[4] Lin N, Xie F, Zhou J, Wu X, Tian W. Corrosion behaviours of P110 steel and chromium coating in CO_2 - saturated simulated oilfield brine. Journal of Wuhan University of Technology - Materials Science Edition, 2011, vol. 26, no. 2, pp. 191-197.

[5] Lin N, Zhou P, Zhou H, Guo J, Zhang H, Zou J, Ma Y, Han P, Tang B. Pack boronizing of P110 oil casing tube steel to combat wear and corrosion. International Journal of Electrochemical Science, 2015, 10, pp. 2694-2706.

[6] Niezgoda T, Miedzińska D, Małek E, Kędzierski P, Sławiński G. Study on carbon dioxide thermodynamic behavior for the purpose of shale rock fracturing, Bulletin of the Polish Academy of Sciences: Technical Sciences, September 2013, vol. 61, issue 3, 1, pp. 605-612.

[7] Revie RW. Oil and Gas Pipelines: Integrity and Safety Handbook, 2015.

[8] Xie R, Gu Z, Yao Y, Xu H, Deng K, Liu Y. Electrochemical study on corrosion behaviours of P110 casing steel in carbon dioxide - saturated oilfield formation water. International Journal of Electrochemical Science, 2015, 10, pp. 5756-5769.

[9] Yin ZF, Wang XZ, Gao RM, Zhang SJ. Electrochemical behaviour and mechanism of CO_2 corrosion on P110 steel in simulated oilfield solution. Anti-Corrosion Methods and Materials, 2011, vol. 58, no. 5, pp. 227-233.

[10] Zhao Z, Qiao G, Tang L, Zhu H, Liao B, Xiao F. Fatigue properties of X80 pipeline steels with ferrite/bainite dual-phase microstructure. Materials Science & Engineering, 2016, A 657, pp. 96-103.